

BACKSUBSTITUTION METHOD FOR SPACECRAFT WITH GENERALLY TRANSLATING APPENDAGES

João Vaz Carneiro*, Peter Johnson† and Hanspeter Schaub‡

While spacecraft have become increasingly complex to satisfy more ambitious mission requirements, simulation tools must be able to replicate their motion numerically. Of particular interest are robotic arms, which are composed of many links modeled as rigid bodies. This work aims to derive the equations of motion of a generally translating component with any number of degrees of freedom and write them using the Backsubstitution Method (BSM). Generalizing the equations for any degree of freedom is beneficial from a dynamics standpoint since it can describe many different components and from a software perspective because the physics modeling is centralized in code. The BSM is used because it is a formulation of the equations suitable for software implementation because of its modularity and speed. Large system mass matrix inversions are avoided while retaining the full nonlinear coupling. Previous work has derived the equations for a general rotating component, while this paper focuses on a translating corollary. First, the kinematics and kinetics are derived and written under the BSM. Then, a realistic numerical simulation is provided to show the impact of the translating component on the spacecraft as it rotates.

NOMENCLATURE

$\mathcal{N}, \mathcal{B}, \mathcal{F}$	= inertial, body and component frames
N, B, F	= origin point for inertial, body and component frames
A_c	= center of mass location of body A
C	= center of mass location of the system
\mathbf{c}	= vector from point B to the center of mass of the spacecraft C , [m]
m_A	= mass of body A, [kg]
$[I_{A,A}]$	= inertia tensor of body A with respect to point A , [kg · m ²]
$\mathbf{r}_{A/B}, \dot{\mathbf{r}}_{A/B}, \ddot{\mathbf{r}}_{A/B}$	= position, inertial velocity and acceleration of point A with respect to B , [m, m/s, m/s ²]
$\sigma_{A/B}$	= attitude of frame A with respect to B expressed in Modified Rodrigues Parameters
$\boldsymbol{\omega}_{A/B}, \dot{\boldsymbol{\omega}}_{A/B}$	= angular velocity and inertial acceleration of frame A with respect to B , [rad/s, rad/s ²]

*Graduate Research Assistant, Ann and H.J. Smead Department of Aerospace Engineering Sciences, University of Colorado, Boulder, 431 UCB, Colorado Center for Astrodynamics Research, Boulder, CO, 80309.

†Undergraduate Research Assistant, Ann and H.J. Smead Department of Aerospace Engineering Sciences, University of Colorado, Boulder, 431 UCB, Colorado Center for Astrodynamics Research, Boulder, CO, 80309.

‡Professor and Department Chair, Schaden Leadership Chair, Ann and H.J. Smead Department of Aerospace Engineering Sciences, University of Colorado, Boulder, 431 UCB, Colorado Center for Astrodynamics Research, Boulder, CO, 80309. AAS Fellow, AIAA Fellow.

$\theta, \dot{\theta}, \ddot{\theta}$	=	hinge's angle, angle rate, and angle acceleration, [rad, rad/s, rad/s ²]
\mathbf{F}_{ext}	=	vector sum of external forces on the spacecraft, [N]
\mathbf{L}_B	=	vector sum of external torques on the spacecraft about point B , [N·m]
u_S	=	scalar torque applied to the hinge, [N·m]
$\dot{\mathbf{a}}, \ddot{\mathbf{a}}$	=	first and second-order time derivatives of vector \mathbf{a} with respect to the inertial frame \mathcal{N}
$\mathbf{a}', \mathbf{a}''$	=	first and second-order time derivatives of vector \mathbf{a} with respect to the body frame \mathcal{B}
$[\tilde{\mathbf{a}}]$	=	cross-product operator written in matrix form
\mathbf{a}_{ij}	=	effector backsubstitution term for $\ddot{\mathbf{r}}_{B/N}$
\mathbf{b}_{ij}	=	effector backsubstitution term for $\dot{\boldsymbol{\omega}}_{B/N}$
\mathbf{c}_{ij}	=	independent effector backsubstitution term
Subscripts		
i	=	i -th component body
sc	=	spacecraft system
hub	=	spacecraft's hub

INTRODUCTION

Spacecraft mission requirements have increasingly required that spacecraft physically interact with other bodies. These include spacecraft-spacecraft interactions for autonomous rendezvous and telerobotic refueling, which is the case for Northrop Grumman's Mission Extension Vehicle¹ and the now-canceled NASA's OSAM-1² mission, but also spacecraft-surface interactions for landing on asteroids or other celestial bodies, which is the case for NASA's OSIRIS-REx mission³ and JAXA's Hayabusa mission.⁴ The spacecraft interaction is done through a translating arm, usually with some damping mechanism for either application. This is particularly evident in the landing missions since the telescopic arm contacts the asteroid to collect samples while dampening the landing and pushing the spacecraft back into orbit. Figure 1 shows a diagram of a spacecraft using a translating appendage for landing or sample collection. These important use cases motivate the need to understand and analyze spacecraft behavior with translating appendages. This work presents an analytic derivation of the equations of motion of spacecraft with these appendages using a general, modular approach.

The field of multibody dynamics is vast and mature. There exist many ways of deriving the equations of motion of a system, namely force and torque-based Newtonian and Eulerian mechanics,⁵ energy-based Lagrangian mechanics,⁶ or Kane's Method.^{7,8} Some formulations use these tools to write the equations in a way that is well suited to aerospace applications, such as Spatial Operator Algebra⁹ (SOA) or the Backsubstitution Method^{10,11} (BSM). This paper focuses on the BSM to formulate the spacecraft equations of motion due to its fast, modular dynamics architecture, which assumes that the spacecraft is composed of a rigid hub to which multiple effectors can be attached in parallel. This tool has been used extensively to model spacecraft components, such as solar arrays,¹² reaction wheels,¹³ VSCMGs,¹⁴ and fuel slosh.¹⁵ Because no cross-coupling terms are ignored, the Backsubstitution method allows for comprehensive simulation testing, guaranteeing that energy and angular momentum are conserved when simulations with conservative forces and torques are performed.

This work aims to derive and implement the equations of motion of a spacecraft with linear translating appendages, also called effectors. These components include landing struts for sample

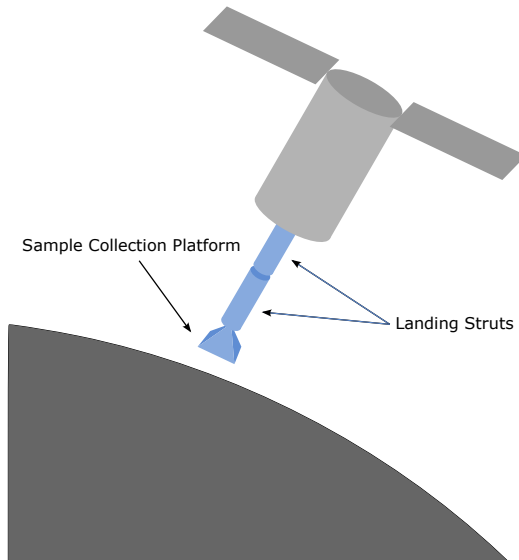


Figure 1: Example of a spacecraft with a translating arm.

collection and landing or even telescoping links deployed after launch. While previous work has derived the equations of motion for particular components, the equations only apply to that specific effector due to the initial assumptions about the mass and geometry properties. Instead, a more general set of equations of motion can be found if no assumptions are made before deriving them. The resulting equations are then applicable to various possible configurations and component properties. This was first introduced in Ref. 16 for single and dual-axis rotating components. It allows multiple different components to be described by the same set of equations of motion since the properties of different components are applied to a general formulation instead of one specific to them. This idea can be further expanded by not limiting the number of degrees of freedom of the component, first introduced in Ref. 17. Each effector can have as many links as needed, resulting in a N -axis formulation for rotation appendages. This work further expands on this work by applying the same concepts to translating components.

This paper is structured as follows. First, the kinematics are derived from the system's problem statement, which includes finding the partial velocities used in Kane's equations. Second, the kinetics are derived using Kane's method, which is especially suitable for deriving complex systems due to its programmatic nature. This is particularly important in this work because the aim is to derive the equations for appendages with any number of degrees of freedom. The equations are derived in the most general way possible, including making no assumptions on mass properties or translation axes. They are then rearranged using the Backsubstitution Method, which includes defining each term needed for this formulation. Finally, an illustrative example that uses the component defined in this paper showcases the coupling and nonlinearities from the equations of motion.

KINEMATICS

Effector Problem Statement

The problem statement for the N -axes translating rigid body effector attached to the hub is given in Figure 2. The inertial frame \mathcal{N} originates at point N . The spacecraft is composed of a rigid hub

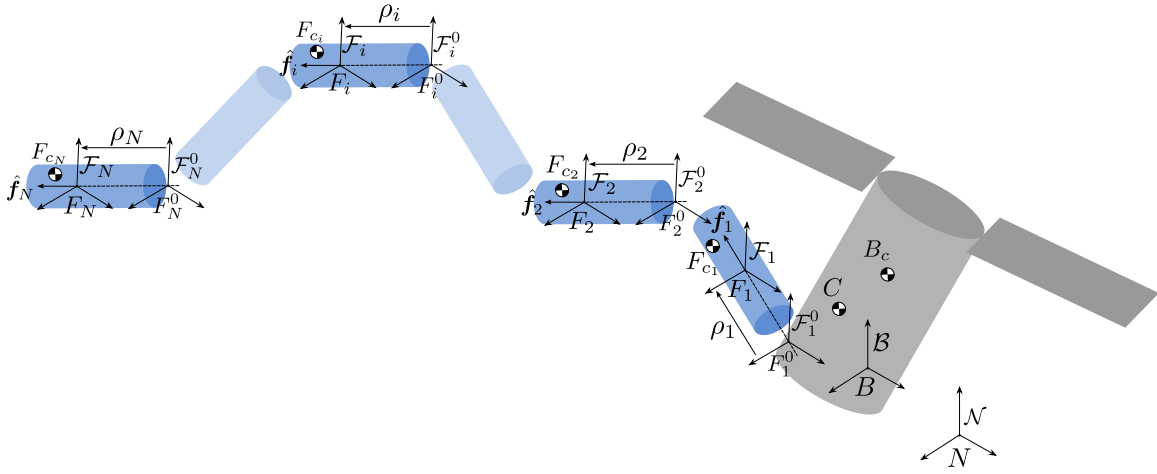


Figure 2: Problem statement for the N -degree-of-freedom translating rigid body.

to which the effector is attached. The B frame has an origin point at B , which does not have to coincide with the center of mass of the hub B_c nor the center of mass of the system C . The hub has mass m_{hub} , center of mass $\mathbf{r}_{B_c/B}$ and inertia about its center of mass $[I_{\text{hub},B_c}]$. The effector consists of a chain of rigid bodies connected through single telescoping axes. The mass and inertia of some bodies can be set to zero to give the axes multiple degrees of freedom of an effector component. Each body has a frame \mathcal{F}_i with origin F_i , mass m_{F_i} , center of mass $\mathbf{r}_{F_{c_i}/F_i}$ and inertia about its center of mass $[I_{F_i,F_{c_i}}]$. The bodies translate about the $\hat{\mathbf{f}}_i$ axis, which passes through the origin of the \mathcal{F}_i frame, with a displacement ρ_i and displacement rate $\dot{\rho}_i$.

Translational Kinematics

The position of the center of mass of the i -th body with respect to the origin of the inertial frame is

$$\begin{aligned}
 \mathbf{r}_{F_{c_i}/N} &= \mathbf{r}_{B/N} + \mathbf{r}_{F_{c_i}/B} \\
 &= \mathbf{r}_{B/N} + \sum_{j=1}^i (\mathbf{r}_{F_j^0/F_{j-1}} + \mathbf{r}_{F_j/F_j^0}) + \mathbf{r}_{F_{c_i}/F_i} \\
 &= \mathbf{r}_{B/N} + \sum_{j=1}^i (\mathbf{r}_{F_j^0/F_{j-1}} + \rho_j \hat{\mathbf{f}}_j) + \mathbf{r}_{F_{c_i}/F_i}
 \end{aligned} \tag{1}$$

where $\mathbf{r}_{F_j/F_j^0} = \rho_j \hat{\mathbf{f}}_j$. The velocity of the center of mass is found by taking the inertial derivative of the position of the center of mass

$$\begin{aligned}
 \dot{\mathbf{r}}_{F_{c_i}/N} &= \dot{\mathbf{r}}_{B/N} + [\tilde{\omega}_{B/N}] \mathbf{r}_{F_{c_i}/B} + \mathbf{r}'_{F_{c_i}/B} \\
 &= \dot{\mathbf{r}}_{B/N} + [\tilde{\omega}_{B/N}] \mathbf{r}_{F_{c_i}/B} + \sum_{j=1}^i \dot{\rho}_j \hat{\mathbf{f}}_j
 \end{aligned} \tag{2}$$

The acceleration is found by taking an inertial derivative again

$$\ddot{\mathbf{r}}_{F_{c_i}/N} = \ddot{\mathbf{r}}_{B/N} - [\tilde{\mathbf{r}}_{F_{c_i}/B}] \dot{\omega}_{B/N} + [\tilde{\omega}_{B/N}] [\tilde{\omega}_{B/N}] \mathbf{r}_{F_{c_i}/B} + 2[\tilde{\omega}_{B/N}] \mathbf{r}'_{F_{c_i}/B} + \mathbf{r}''_{F_{c_i}/B}$$

$$= \ddot{\mathbf{r}}_{B/N} - [\tilde{\mathbf{r}}_{F_{c_i}/B}] \dot{\boldsymbol{\omega}}_{B/N} + [\tilde{\boldsymbol{\omega}}_{B/N}] [\tilde{\boldsymbol{\omega}}_{B/N}] \mathbf{r}_{F_{c_i}/B} + 2[\tilde{\boldsymbol{\omega}}_{B/N}] \mathbf{r}'_{F_{c_i}/B} + \sum_{j=1}^i \rho_j \hat{\mathbf{f}}_j \quad (3)$$

Rotational Kinematics

The rotational kinematics for this problem are trivial because each body does not rotate with respect to the hub. Therefore, the angular velocity and angular acceleration of the i -th body are

$$\boldsymbol{\omega}_{\mathcal{F}_i/N} = \boldsymbol{\omega}_{B/N} \quad (4)$$

$$\dot{\boldsymbol{\omega}}_{\mathcal{F}_i/N} = \dot{\boldsymbol{\omega}}_{B/N} \quad (5)$$

Partial Velocities

The partial velocities^{5,7} are computed by taking the partial derivative of each body's center of mass velocity $\dot{\mathbf{r}}_{F_{c_i}/N}$ or the frame's angular velocity $\boldsymbol{\omega}_{\mathcal{F}_i/N}$ with respect to each generalized coordinate u_r . Therefore, each entry applies $\partial/\partial r_i$ to the corresponding variable, where 1-3 is for $\mathbf{r}_{B/N}$, 4-6 is for $\boldsymbol{\omega}_{B/N}$ and the rest are for all θ_i . The partial velocity table is shown in Table 1.

Table 1: Partial velocities.

r	$[\mathbf{v}_r^{Bc}]$	$[\boldsymbol{\omega}_r^B]$	$[\mathbf{v}_r^{F_{c_1}}]$	$[\boldsymbol{\omega}_r^{\mathcal{F}_1}]$	$[\mathbf{v}_r^{F_{c_2}}]$	$[\boldsymbol{\omega}_r^{\mathcal{F}_2}]$...	$[\mathbf{v}_r^{F_{c_i}}]$	$[\boldsymbol{\omega}_r^{\mathcal{F}_i}]$...	$[\mathbf{v}_r^{F_{c_N}}]$	$[\boldsymbol{\omega}_r^{\mathcal{F}_N}]$
1 – 3	$[I_{3 \times 3}]$	$[0_{3 \times 3}]$	$[I_{3 \times 3}]$	$[0_{3 \times 3}]$	$[I_{3 \times 3}]$	$[0_{3 \times 3}]$...	$[I_{3 \times 3}]$	$[0_{3 \times 3}]$...	$[I_{3 \times 3}]$	$[0_{3 \times 3}]$
4 – 6	$-\tilde{[\mathbf{r}_{Bc/B}]}$	$[I_{3 \times 3}]$	$-\tilde{[\mathbf{r}_{F_{c_1}/B}]}$	$[I_{3 \times 3}]$	$-\tilde{[\mathbf{r}_{F_{c_2}/B}]}$	$[I_{3 \times 3}]$...	$-\tilde{[\mathbf{r}_{F_{c_i}/B}]}$	$[I_{3 \times 3}]$...	$-\tilde{[\mathbf{r}_{F_{c_N}/B}]}$	$[I_{3 \times 3}]$
7	$[0_{3 \times 1}]$	$[0_{3 \times 1}]$	$\hat{\mathbf{f}}_1$	$[0_{3 \times 1}]$	$\hat{\mathbf{f}}_1$	$[0_{3 \times 1}]$...	$\hat{\mathbf{f}}_1$	$[0_{3 \times 1}]$...	$\hat{\mathbf{f}}_1$	$[0_{3 \times 1}]$
8	$[0_{3 \times 1}]$	$[0_{3 \times 1}]$	$[0_{3 \times 1}]$	$[0_{3 \times 1}]$	$\hat{\mathbf{f}}_2$	$[0_{3 \times 1}]$...	$\hat{\mathbf{f}}_2$	$[0_{3 \times 1}]$...	$\hat{\mathbf{f}}_2$	$[0_{3 \times 1}]$
\vdots	\vdots	\vdots	\vdots	\vdots	\vdots	\vdots	\ddots	\vdots	\vdots	\ddots	\vdots	\vdots
$6 + i$	$[0_{3 \times 1}]$	$[0_{3 \times 1}]$	$[0_{3 \times 1}]$	$[0_{3 \times 1}]$	$[0_{3 \times 1}]$	$[0_{3 \times 1}]$...	$\hat{\mathbf{f}}_i$	$[0_{3 \times 1}]$...	$\hat{\mathbf{f}}_i$	$[0_{3 \times 1}]$
\vdots	\vdots	\vdots	\vdots	\vdots	\vdots	\vdots	\ddots	\vdots	\vdots	\ddots	\vdots	\vdots
$6 + N$	$[0_{3 \times 1}]$	$[0_{3 \times 1}]$	$[0_{3 \times 1}]$	$[0_{3 \times 1}]$	$[0_{3 \times 1}]$	$[0_{3 \times 1}]$...	$[0_{3 \times 1}]$	$[0_{3 \times 1}]$...	$\hat{\mathbf{f}}_N$	$[0_{3 \times 1}]$

KINETICS

Translation Equations of Motion

The general active force for the system's translation is

$$\mathbf{F}_{1-3} = F_{\text{ext}} \quad (6)$$

and the general inertia force is

$$\mathbf{F}_{1-3}^* = - \sum_{i=0}^N m_{F_i} [\mathbf{v}_{1-3}^{F_{c_i}}]^T \ddot{\mathbf{r}}_{F_{c_i}/N} \quad (7)$$

where $[\mathbf{v}_{1-3}^{F_{c_i}}]$ is the identity matrix as defined in the partial velocity table. Substituting in the known values into $\mathbf{F}_{1-3} + \mathbf{F}_{1-3}^* = \mathbf{0}$ yields the following

$$\begin{aligned} \sum_{i=0}^N m_{F_i} \ddot{\mathbf{r}}_{B/N} - \sum_{i=0}^N m_{F_i} [\tilde{\mathbf{r}}_{F_{c_i}/B}] \dot{\boldsymbol{\omega}}_{B/N} + \sum_{i=1}^N \sum_{j=1}^i m_{F_i} \ddot{\rho}_j \hat{\mathbf{f}}_j = \mathbf{F}_{\text{ext}} \\ - \sum_{i=0}^N m_{F_i} [\tilde{\boldsymbol{\omega}}_{B/N}] [\tilde{\boldsymbol{\omega}}_{B/N}] \mathbf{r}_{F_{c_i}/B} - \sum_{i=0}^N 2m_{F_i} [\tilde{\boldsymbol{\omega}}_{B/N}] \mathbf{r}'_{F_{c_i}/B} \end{aligned} \quad (8)$$

Before proceeding, the following equalities are used

$$m_{\text{sc}} = \sum_{i=0}^N m_{F_i}, \quad m_{\text{sc}} \mathbf{c} = \sum_{i=0}^N m_{F_i} \mathbf{r}_{F_{c_i}/B}, \quad m_{\text{sc}} \mathbf{c}' = \sum_{i=0}^N m_{F_i} \mathbf{r}'_{F_{c_i}/B} \quad (9)$$

Having a single sum of the $\ddot{\rho}_i \hat{\mathbf{f}}_i$ terms is also beneficial. We can use the following property to achieve that

$$\sum_{i=1}^N \sum_{j=1}^i f_{ij} = \sum_{i=1}^N \sum_{j=i}^N f_{ji} \quad (10)$$

After these simplifications and rearrangements, we get

$$m_{\text{sc}} \ddot{\mathbf{r}}_{B/N} - m_{\text{sc}} [\tilde{\mathbf{c}}] \dot{\boldsymbol{\omega}}_{B/N} + \sum_{i=1}^N \left(\sum_{j=i}^N m_{F_j} \right) \ddot{\rho}_i \hat{\mathbf{f}}_i = \mathbf{F}_{\text{ext}} - 2m_{\text{sc}} [\tilde{\boldsymbol{\omega}}_{B/N}] \mathbf{c}' - m_{\text{sc}} [\tilde{\boldsymbol{\omega}}_{B/N}] [\tilde{\boldsymbol{\omega}}_{B/N}] \mathbf{c} \quad (11)$$

Rotational Equations of Motion

The general active force for the system's rotation is

$$\mathbf{F}_{4-6} = \mathbf{L}_B \quad (12)$$

and the general inertia force is

$$\mathbf{F}_{4-6}^* = - \sum_{i=0}^N (m_{F_i} [\mathbf{v}_{4-6}^{F_{c_i}}]^T \ddot{\mathbf{r}}_{F_{c_i}/N} + [\boldsymbol{\omega}_{4-6}^{F_i}]^T ([I_{S_i, F_{c_i}}] \dot{\boldsymbol{\omega}}_{B/N} + [\tilde{\boldsymbol{\omega}}_{B/N}] [I_{S_i, F_{c_i}}] \boldsymbol{\omega}_{B/N})) \quad (13)$$

where $[\mathbf{v}_{4-6}^{F_{c_i}}] = -[\tilde{\mathbf{r}}_{F_{c_i}/B}]$ and $[\boldsymbol{\omega}_{4-6}^{F_i}]$ is the identity matrix. Substituting in the known values into $\mathbf{F}_{4-6} + \mathbf{F}_{4-6}^* = \mathbf{0}$ yields the following

$$\begin{aligned} m_{\text{sc}} [\tilde{\mathbf{c}}] \ddot{\mathbf{r}}_{B/N} + \sum_{i=0}^N \left([I_{F_i, F_{c_i}}] - m_{F_i} [\tilde{\mathbf{r}}_{F_{c_i}/B}] [\tilde{\mathbf{r}}_{F_{c_i}/B}] \right) \dot{\boldsymbol{\omega}}_{B/N} + \sum_{i=1}^N \sum_{j=1}^i m_{F_i} [\tilde{\mathbf{r}}_{F_{c_i}/B}] \ddot{\rho}_j \hat{\mathbf{f}}_j \\ = \mathbf{L}_B - \sum_{i=0}^N m_{F_i} [\tilde{\mathbf{r}}_{F_{c_i}/B}] [\tilde{\boldsymbol{\omega}}_{B/N}] [\tilde{\boldsymbol{\omega}}_{B/N}] \mathbf{r}_{F_{c_i}/B} - \sum_{i=0}^N 2m_{F_i} [\tilde{\mathbf{r}}_{F_{c_i}/B}] [\tilde{\boldsymbol{\omega}}_{B/N}] \mathbf{r}'_{F_{c_i}/B} \end{aligned}$$

$$- \sum_{i=0}^N [\tilde{\omega}_{\mathcal{B}/\mathcal{N}}] [I_{F_i, F_{c_i}}] \omega_{\mathcal{B}/\mathcal{N}} \quad (14)$$

The triple cross product identity $\mathbf{a} \times (\mathbf{b} \times \mathbf{c}) = (\mathbf{a} \times \mathbf{b}) \times \mathbf{c} + \mathbf{b} \times (\mathbf{a} \times \mathbf{c})$ are used to rearrange the following terms.

$$[\tilde{\mathbf{r}}_{F_{c_i}/B}] [\tilde{\omega}_{\mathcal{B}/\mathcal{N}}] [\tilde{\omega}_{\mathcal{B}/\mathcal{N}}] \mathbf{r}_{F_{c_i}/B} = -[\tilde{\omega}_{\mathcal{B}/\mathcal{N}}] [\tilde{\mathbf{r}}_{F_{c_i}/B}] [\tilde{\mathbf{r}}_{F_{c_i}/B}] \omega_{\mathcal{B}/\mathcal{N}} \quad (15)$$

$$[\tilde{\mathbf{r}}_{F_{c_i}/B}] [\tilde{\omega}_{\mathcal{B}/\mathcal{N}}] \mathbf{r}'_{F_{c_i}/B} = -[\tilde{\mathbf{r}}'_{F_{c_i}/B}] [\tilde{\mathbf{r}}_{F_{c_i}/B}] \omega_{\mathcal{B}/\mathcal{N}} + [\tilde{\omega}_{\mathcal{B}/\mathcal{N}}] [\tilde{\mathbf{r}}_{F_{c_i}/B}] \mathbf{r}'_{F_{c_i}/B} \quad (16)$$

These can be used to group terms and simplify along with the system inertia definitions below.

$$[I_{sc,B}] = \sum_{i=0}^N ([I_{F_i, F_{c_i}}] - m_{F_i} [\tilde{\mathbf{r}}_{F_{c_i}/B}] [\tilde{\mathbf{r}}_{F_{c_i}/B}]) \quad (17)$$

$$[I'_{sc,B}] = - \sum_{i=0}^N m_{F_i} ([\tilde{\mathbf{r}}_{F_{c_i}/B}] [\tilde{\mathbf{r}}'_{F_{c_i}/B}] + [\tilde{\mathbf{r}}'_{F_{c_i}/B}] [\tilde{\mathbf{r}}_{F_{c_i}/B}]) \quad (18)$$

After simplifying and rearranging, the final equation for rotational motion is

$$m_{sc} [\tilde{\mathbf{c}}] \ddot{\mathbf{r}}_{B/\mathcal{N}} + [I_{sc,B}] \dot{\omega}_{\mathcal{B}/\mathcal{N}} + \sum_{i=1}^N \left(\sum_{j=i}^N m_{F_j} [\tilde{\mathbf{r}}_{F_{c_j}/B}] \right) \ddot{\rho}_i \hat{\mathbf{f}}_i = \mathbf{L}_B - [\tilde{\omega}_{\mathcal{B}/\mathcal{N}}] [I_{sc,B}] \omega_{\mathcal{B}/\mathcal{N}} - [I'_{sc,B}] \omega_{\mathcal{B}/\mathcal{N}} - \sum_{i=1}^N m_{F_i} [\tilde{\omega}_{\mathcal{B}/\mathcal{N}}] [\tilde{\mathbf{r}}_{F_{c_i}/B}] \mathbf{r}'_{F_{c_i}/B} \quad (19)$$

N-th Translating Body Equations of Motion

The general active force for the N-th body is

$$\mathbf{F}_n = u_n \quad (20)$$

and the general inertia force is

$$\mathbf{F}_n^* = - \sum_{i=0}^N \hat{\mathbf{f}}_n^T \ddot{\mathbf{r}}_{F_{c_i}/\mathcal{N}} \quad (21)$$

After using Kane's equation and plugging in the result from Equation 3, the effector equation for the i -th body is

$$\begin{aligned} \hat{\mathbf{f}}_n^T \sum_{i=1}^n \left(\sum_{j=n}^N m_{F_j} \right) \ddot{\rho}_i \hat{\mathbf{f}}_i + \hat{\mathbf{f}}_n^T \sum_{i=n+1}^N \left(\sum_{j=i}^N m_{F_j} \right) \ddot{\rho}_i \hat{\mathbf{f}}_i &= u_n \\ - \hat{\mathbf{f}}_n^T \sum_{i=n}^N m_{F_i} \ddot{\mathbf{r}}_{B/\mathcal{N}} + \hat{\mathbf{f}}_n^T \sum_{i=n}^N m_{F_i} [\tilde{\mathbf{r}}_{F_{c_i}/B}] \dot{\omega}_{\mathcal{B}/\mathcal{N}} \\ - \hat{\mathbf{f}}_n^T \sum_{i=n}^N m_{F_i} [\tilde{\omega}_{\mathcal{B}/\mathcal{N}}] [\tilde{\omega}_{\mathcal{B}/\mathcal{N}}] \mathbf{r}_{F_{c_i}/B} - \hat{\mathbf{f}}_n^T \sum_{i=n}^N 2m_{F_i} [\tilde{\omega}_{\mathcal{B}/\mathcal{N}}] \mathbf{r}'_{F_{c_i}/B} & \quad (22) \end{aligned}$$

BACKSUBSTITUTION METHOD IMPLEMENTATION

The Backsubstitution Method¹⁰ arranges the equations of motion into a specific form to avoid inverting the entire system's mass matrix. Under the assumption that the spacecraft comprises a rigid hub with multiple parallel components, the system's mass matrix has a form that can be leveraged to invert smaller portions of it instead. The general structure of the mass matrix under these assumptions is presented in Equation 23.

$$\begin{bmatrix}
 [\cdot]_{3 \times 3} & [\cdot]_{3 \times 3} & [\cdot]_{3 \times N_1} & [\cdot]_{3 \times N_2} & \cdots & [\cdot]_{3 \times N_e} \\
 [\cdot]_{3 \times 3} & [\cdot]_{3 \times 3} & [\cdot]_{3 \times N_1} & [\cdot]_{3 \times N_2} & \cdots & [\cdot]_{3 \times N_e} \\
 [\cdot]_{N_1 \times 3} & [\cdot]_{N_1 \times 3} & [\cdot]_{N_1 \times N_1} & [0]_{N_1 \times N_2} & \cdots & [0]_{N_1 \times N_e} \\
 [\cdot]_{N_2 \times 3} & [\cdot]_{N_2 \times 3} & [0]_{N_2 \times N_1} & [\cdot]_{N_2 \times N_2} & \cdots & [0]_{N_2 \times N_e} \\
 \vdots & \vdots & \vdots & \vdots & \ddots & \vdots \\
 [\cdot]_{N_e \times 3} & [\cdot]_{N_e \times 3} & [0]_{N_e \times N_1} & [0]_{N_e \times N_2} & \cdots & [\cdot]_{N_e \times N_e}
 \end{bmatrix}
 \begin{bmatrix}
 \ddot{\mathbf{r}}_{B/N} \\
 \dot{\boldsymbol{\omega}}_{B/N} \\
 \boldsymbol{\alpha}_1 \\
 \boldsymbol{\alpha}_2 \\
 \vdots \\
 \boldsymbol{\alpha}_e
 \end{bmatrix}
 =
 \begin{bmatrix}
 [\cdot]_{3 \times 1} \\
 [\cdot]_{3 \times 1} \\
 [\cdot]_{N_1 \times 1} \\
 [\cdot]_{N_2 \times 1} \\
 \vdots \\
 [\cdot]_{N_e \times 1}
 \end{bmatrix}
 \quad (23)$$

The mass matrix has a special structure where the first six rows and six columns are fully populated, along with the main block diagonal. This is a consequence of the spacecraft's geometry with a centralized hub and multiple parallel effectors that do not directly depend on each other. Therefore, only a 6x6 matrix of the hub's translation and rotation states must be inverted, along with any mass matrices for each subcomponent. This yields a set of equations that is particularly suitable for implementation in software because inverting matrices scales with the cube of the matrix dimension. Moreover, the implementation is completely modular, as any number of effectors can be added in parallel without changing the form of the equations.

Using the Backsubstitution Method, the effector equations are written like

$$[\mathbf{M}_\alpha] \ddot{\boldsymbol{\alpha}} = [\mathbf{A}_\alpha^*] \ddot{\mathbf{r}}_{B/N} + [\mathbf{B}_\alpha^*] \dot{\boldsymbol{\omega}}_{B/N} + [\mathbf{C}_\alpha^*] \quad (24)$$

where $[\mathbf{M}_\alpha]$ is the mass matrix and $\ddot{\boldsymbol{\alpha}}$ is the stacked vector of states for the effector. The system's translational and rotational equations are coupled and can be written as

$$\begin{bmatrix}
 [A] & [B] \\
 [C] & [D]
 \end{bmatrix}
 \begin{bmatrix}
 \ddot{\mathbf{r}}_{B/N} \\
 \dot{\boldsymbol{\omega}}_{B/N}
 \end{bmatrix}
 =
 \begin{bmatrix}
 \mathbf{v}_{\text{Trans}} \\
 \mathbf{v}_{\text{Rot}}
 \end{bmatrix}
 \quad (25)$$

In this section, the backsubstitution contributions from the N -axis translating component are defined, starting with the effector's mass matrix $[\mathbf{M}_\rho]$

$$\mathbf{M}_{\rho_{n,i}} = \begin{cases} \hat{\mathbf{f}}_n^T \left(\sum_{j=n}^N m_{F_j} \right) \hat{\mathbf{f}}_i, & i \leq n \\ \hat{\mathbf{f}}_n^T \left(\sum_{j=i}^N m_{F_j} \right) \hat{\mathbf{f}}_i, & i > n \end{cases} \quad (26)$$

The $[\mathbf{A}^*]$, $[\mathbf{B}^*]$, and $[\mathbf{C}^*]$ can be pulled from the N^{th} body formulation

$$\mathbf{A}_{\rho_n}^* = -\hat{\mathbf{f}}_n^T \sum_{i=n}^N m_{F_i} \quad (27)$$

$$\mathbf{B}_{\rho_n}^* = \hat{\mathbf{f}}_n^T \sum_{i=n}^N m_{F_i} [\tilde{\mathbf{r}}_{F_{c_i}/B}] \quad (28)$$

$$\mathbf{C}_{\rho_n}^* = u_n - \hat{\mathbf{f}}_n^T \sum_{i=n}^N m_{F_i} [\tilde{\boldsymbol{\omega}}_{B/N}] [\tilde{\boldsymbol{\omega}}_{B/N}] \mathbf{r}_{F_{c_i}/B} - \hat{\mathbf{f}}_n^T \sum_{i=n}^N 2m_{F_i} [\tilde{\boldsymbol{\omega}}_{B/N}] \mathbf{r}'_{F_{c_i}/B} \quad (29)$$

With these and the translation and rotation equations of motion, the $[A]$, $[B]$, $[C]$ and $[D]$ matrices are defined

$$[A] = m_{\text{sc}} [I_{3 \times 3}] + \sum_{i=1}^N \left(\sum_{j=i}^N m_{F_j} \right) \hat{\mathbf{f}}_i \mathbf{A}_{\rho_i} \quad (30)$$

$$[B] = -m_{\text{sc}} [\tilde{\mathbf{c}}] + \sum_{i=1}^N \left(\sum_{j=i}^N m_{F_j} \right) \hat{\mathbf{f}}_i \mathbf{B}_{\rho_i} \quad (31)$$

$$[C] = m_{\text{sc}} [\tilde{\mathbf{c}}] + \sum_{i=1}^N \left(\sum_{j=i}^N m_{F_j} [\tilde{\mathbf{r}}_{F_{c_j}/B}] \right) \hat{\mathbf{f}}_i \mathbf{A}_{\rho_i} \quad (32)$$

$$[D] = [I_{\text{sc},B}] + \sum_{i=1}^N \left(\sum_{j=i}^N m_{F_j} [\tilde{\mathbf{r}}_{F_{c_j}/B}] \right) \hat{\mathbf{f}}_i \mathbf{B}_{\rho_i} \quad (33)$$

The definitions for $\mathbf{v}_{\text{Trans}}$ and \mathbf{v}_{Rot} complete the backsubstitution formulation matrix

$$\mathbf{v}_{\text{Trans}} = \mathbf{F}_{\text{ext}} - 2m_{\text{sc}} [\tilde{\boldsymbol{\omega}}_{B/N}] \mathbf{c}' - m_{\text{sc}} [\tilde{\boldsymbol{\omega}}_{B/N}] [\tilde{\boldsymbol{\omega}}_{B/N}] \mathbf{c} - \sum_{i=1}^N \left(\sum_{j=i}^N m_{F_j} \right) \hat{\mathbf{f}}_i \mathbf{C}_{\rho_i} \quad (34)$$

$$\begin{aligned} \mathbf{v}_{\text{Rot}} = & \mathbf{L}_B - [\tilde{\boldsymbol{\omega}}_{B/N}] [I_{\text{sc},B}] \boldsymbol{\omega}_{B/N} - [I'_{\text{sc},B}] \boldsymbol{\omega}_{B/N} \\ & - \sum_{i=1}^N m_{F_i} [\tilde{\boldsymbol{\omega}}_{B/N}] [\tilde{\mathbf{r}}_{F_{c_i}/B}] \mathbf{r}'_{F_{c_i}/B} - \sum_{i=1}^N \left(\sum_{j=i}^N m_{F_j} [\tilde{\mathbf{r}}_{F_{c_j}/B}] \right) \hat{\mathbf{f}}_i \mathbf{C}_{\rho_i} \end{aligned} \quad (35)$$

NUMERICAL SIMULATION

This section provides an example of the N -axis translating effector in a realistic simulation. The spacecraft comprises a rigid hub with a four-link appendage. The scenario starts with the links stowed at their nominal position and the spacecraft rotating in space. Then, each link extends, deploying the effector to full extension. The goal is to show the impact of the change in inertia due to the appendage deployment on the system's angular velocity. Figure 3 shows the spacecraft with the component in the extended configuration.

The system's initial conditions for both simulations are identical and shown in Table 2.

The hub's mass properties are shown in Table 3. Each link's mass and geometry properties are shown in Table 4.

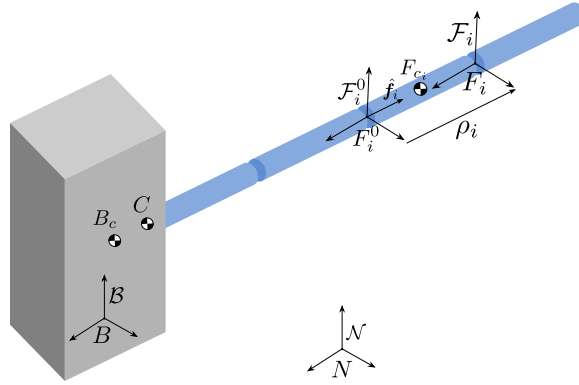


Figure 3: Diagram of the spacecraft in the extended position.

Table 2: Spacecraft initial conditions.

Parameter	Notation	Value	Units
Semi-major Axis	a	8000	km
Eccentricity	e	0.1	-
Inclination	i	0	deg
Longitude of the Ascending Node	Ω	0	deg
Argument of Periapsis	ω	0	deg
Initial True Anomaly	f	0	deg

Table 3: Simulation parameters for the rigid hub.

Parameter	Notation	Value	Units
Hub's mass	m_{hub}	400	kg
Hub's inertia about the hub's center of mass	${}^{\mathcal{B}}[I_{\text{hub}, B_c}]$	${}^{\mathcal{B}} \begin{bmatrix} 1500 & 0 & 0 \\ 0 & 1500 & 0 \\ 0 & 0 & 600 \end{bmatrix}$	$\text{kg} \cdot \text{m}^2$
Hub's center of mass location with respect to B	${}^{\mathcal{B}}\mathbf{r}_{B_c/B}$	${}^{\mathcal{B}}[0, 0, 0]^T$	m

Table 4: Simulation parameters for the robotic arm simulation.

Parameter	Notation	Value	Units
Link's mass	m_{F_i}	100	kg
Link's inertia about its center of mass	${}^{\mathcal{F}_1}[I_{F_i, F_{c_i}}]$	$\begin{bmatrix} 77.25 & 0 & 0 \\ 0 & 0.75 & 0 \\ 0 & 0 & 77.25 \end{bmatrix}$	$\text{kg} \cdot \text{m}^2$
Link's center of mass location with respect to hinge point	${}^{\mathcal{F}_i}\mathbf{r}_{F_{c_i}/F_i}$	${}^{\mathcal{F}_i}[0, 1.5, 0]^T$	m
Position between hinge points	${}^{\mathcal{F}_i}\mathbf{r}_{F_i^0/F_{i-1}}$	${}^{\mathcal{F}_i}[0, 3, 0]^T$	m
Translating axis	${}^{\mathcal{F}_i}\hat{\mathbf{f}}_i$	${}^{\mathcal{F}_i}[0, 1, 0]^T$	–
Linear spring constant	k_i	500	N·m/rad
Linear damper constant	c_i	3000	N·m/rad

The time history for all displacement and displacement rates are shown in Figure 4. The displacements start at their nominal position of zero. The first link does not move, so its displacement remains nominal. The other links extend out until they have moved a distance equal to its length of 3 meters. The profilers assume a constant acceleration, so the displacement rates are mostly linear. A smoothing factor is applied when the profilers change from positive to negative acceleration. Note that the displacement rates show some oscillations; these can be explained by the spring and damper used to track the reference displacement and displacement rates provided by the profilers.

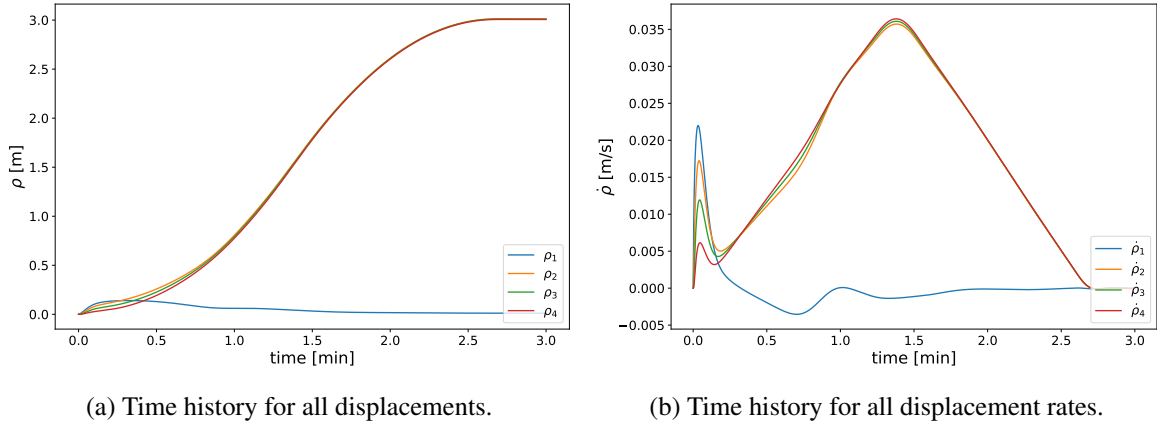


Figure 4: Time history of the effector states.

The time history for the hub's attitude, expressed in Modified Rodrigues Parameters,⁵ and angular

velocity is shown in Figure 5. Looking at Figure 5b, the norm of the angular velocity falls as the simulation progresses, which coincides with the deployment of the appendage. This is the expected behavior and can be explained through the conservation of angular momentum. Since no external torques act on the spacecraft, its angular momentum must be conserved. Let us define the angular momentum as $\mathbf{H} = [I]\boldsymbol{\omega}$, where $[I]$ is the inertia and $\boldsymbol{\omega}$ is the angular velocity. When the links move away from the system’s center of mass, the spacecraft’s inertia $[I]$ increases; hence, the angular velocity $\boldsymbol{\omega}$ must decrease to maintain the same value of \mathbf{H} . It is expected that the attitude rate does not decrease linearly since the inertia can be fully populated, adding non-diagonal terms.

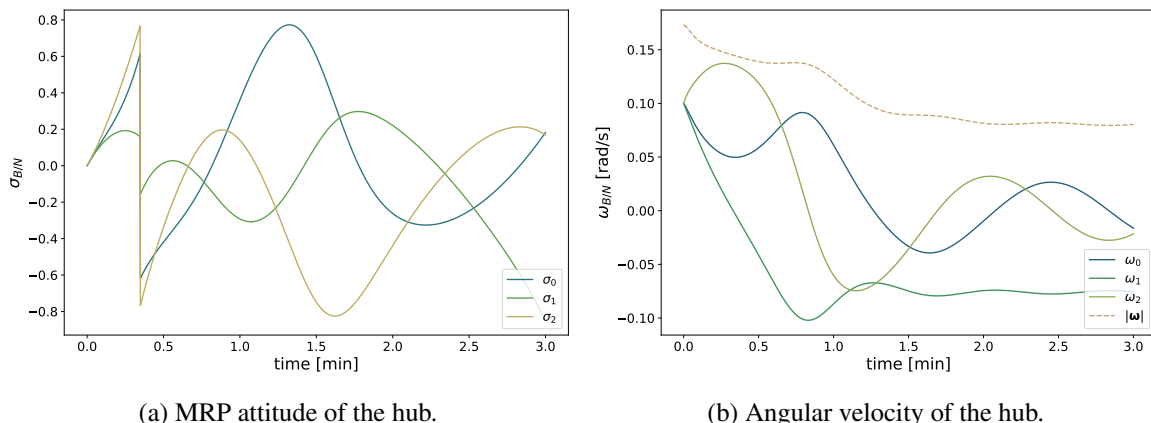


Figure 5: Time history for the hub’s states with a robotic arm.

CONCLUSION

This work shows the analytic derivation of a spacecraft’s fully coupled equations of motion with a translating appendage consisting of any number of links. No mass or geometry assumptions are made on the equations, which yields a general set of equations that can describe a wide range of configurations for the translating appendage. Given the mathematical development provided, a numerical simulation demonstrates a realistic use case for this component.

ACKNOWLEDGMENTS

This work was supported by the La Caixa Foundation (ID 100010434) through the Postgraduate Fellowships Abroad program under agreement LCF/BQ/EU22/11930093.

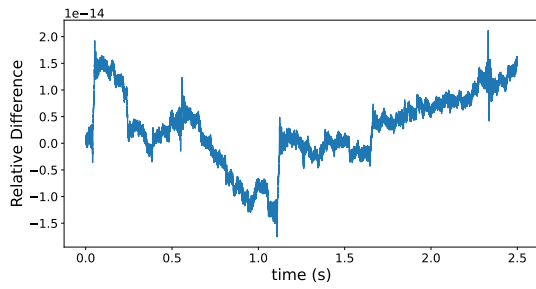
REFERENCES

- [1] N. T. Redd, “Bringing satellites back from THE DEAD: Mission extension vehicles give defunct spacecraft a new lease on life,” *IEEE Spectrum*, Vol. 57, 2020, pp. 6–7.
- [2] M. A. Shoemaker, M. Vavrina, D. E. Gaylor, R. McIntosh, M. Volle, and J. Jacobsohn, “OSAM-1 decommissioning orbit design,” *AAS/AIAA Astrodynamics Specialist Conference*, 2020.
- [3] K. Berry, B. Sutter, A. May, K. Williams, B. W. Barbee, M. Beckman, and B. Williams, “OSIRIS-REx touch-and-go (TAG) mission design and analysis,” *36th Annual AAS Guidance and Control Conference*, No. GSFC. CP. 7566.2013, 2013.
- [4] J. Kawaguchi, A. Fujiwara, and T. Uesugi, “Hayabusa—Its technology and science accomplishment summary and Hayabusa-2,” *Acta Astronautica*, Vol. 62, No. 10-11, 2008, pp. 639–647.
- [5] H. Schaub and J. L. Junkins, *Analytical Mechanics of Space Systems*. Reston, VA: AIAA Education Series, 4th ed., 2018, 10.2514/4.105210.

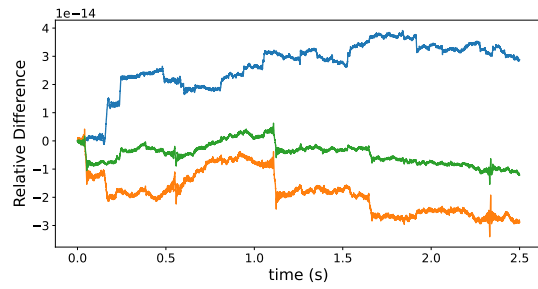
- [6] M. Géradin and D. J. Rixen, *Mechanical vibrations: theory and application to structural dynamics*. John Wiley & Sons, 2014.
- [7] T. R. Kane and D. A. Levinson, *Dynamics, theory and applications*. McGraw Hill, 1985.
- [8] C. M. Roithmayr and D. H. Hodges, “Dynamics: theory and application of Kane’s method,” 2016.
- [9] A. Jain, *Robot and Multibody Dynamics: Analysis and Algorithms*. Springer Science & Business Media, 2010.
- [10] C. Allard, M. Diaz-Ramos, P. W. Kenneally, H. Schaub, and S. Piggott, “Modular Software Architecture for Fully-Coupled Spacecraft Simulations,” *Journal of Aerospace Information Systems*, Vol. 15, No. 12, 2018, pp. 670–683, 10.2514/1.I010653.
- [11] C. Allard, M. Diaz-Ramos, and H. Schaub, “Computational Performance of Complex Spacecraft Simulations Using Back-Substitution,” *Journal Of Aerospace Information Systems*, Vol. 16, Oct. 2019, pp. 427–436, 10.2514/1.I010713.
- [12] C. Allard, H. Schaub, and S. Piggott, “General Hinged Solar Panel Dynamics Approximating First-Order Spacecraft Flexing,” *AIAA Journal of Spacecraft and Rockets*, Vol. 55, No. 5, 2018, pp. 1290–1298, 10.2514/1.A34125.
- [13] J. Alcorn, C. Allard, and H. Schaub, “Fully Coupled Reaction Wheel Static and Dynamic Imbalance for Spacecraft Jitter Modeling,” *AIAA Journal of Guidance, Control, and Dynamics*, Vol. 41, No. 6, 2018, pp. 1380–1388, 10.2514/1.G003277.
- [14] J. Alcorn, C. Allard, and H. Schaub, “Fully-Coupled Dynamical Jitter Modeling Of Variable-Speed Control Moment Gyroscopes,” *AAS/AIAA Astrodynamics Specialist Conference*, Stevenson, WA, Aug. 20–24 2017. Paper No. AAS-17-730.
- [15] P. Panicucci, C. Allard, and H. Schaub, “Spacecraft Dynamics Employing a General Multi-tank and Multi-thruster Mass Depletion Formulation,” *Journal of Astronautical Sciences*, Vol. 65, No. 4, 2018, pp. 423–447, 10.1007/s40295-018-0133-0.
- [16] J. Vaz Carneiro, C. Allard, and H. Schaub, “Rotating Rigid Body Dynamics Architecture For Spacecraft Simulation Software Implementation,” *AAS Guidance and Control Conference*, Breckenridge, CO, Feb. 2–8 2023. Paper No. AAS-23-112.
- [17] J. Vaz Carneiro, C. Allard, and H. Schaub, “Effector Dynamics For Sequentially Rotating Rigid Body Spacecraft Components,” *AAS/AIAA Astrodynamics Specialist Conference*, Big Sky, MO, Aug. 13–17 2023. Paper AAS 23–192.

APPENDIX

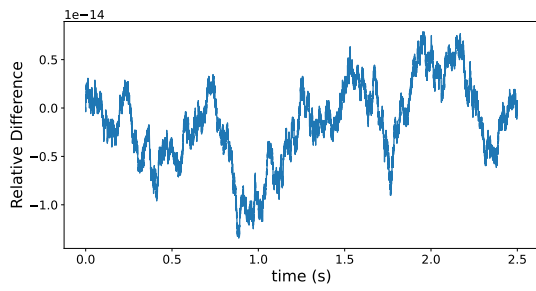
The equations of motion are verified by running a simulation of a spacecraft with a translating appendage of four links. The component’s geometry is chosen to exercise all the nonlinearities of the system, i.e., no special configuration is used that would simplify the equations. The simulation is run in a conservative environment, which means only conservative forces and torques are present, which, in this case, consist of gravity only. The spacecraft’s energy and angular momentum must be conserved in a conservative environment. These two quantities can be separated further into their orbital and rotational parts, which means four quantities must be conserved throughout the simulation. This is verified by computing their value at all timesteps and comparing the relative difference to the initial values. The results are shown in Figure 6, which shows that the relative difference is on the order of 10^{-14} , corresponding to machine precision. The random walk is characteristic of fixed timestep integrators, which the fourth-order Runge-Kutta integrator is part of.



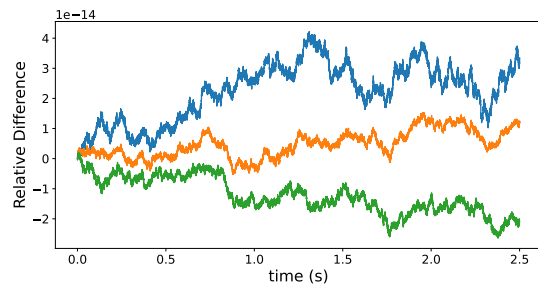
(a) Orbital energy.



(b) Orbital angular momentum.



(c) Rotational energy.



(d) Rotational angular momentum.

Figure 6: Conservation plots for module verification.